

Looking for the Wind in the Dust

S. C. Gallagher,¹ J. E. Everett,² S. K. Keating,³ A. R. Hill,¹ and R. P. Deo¹

¹*University of Western Ontario, Department of Physics & Astronomy*

²*University of Wisconsin, Department of Physics*

³*University of Toronto, Department of Astronomy*

Abstract. The blue-shifted broad emission lines and/or broad absorption lines seen in many luminous quasars are striking evidence for a broad line region in which radiation driving plays an important role. We consider the case for a similar role for radiation driving beyond the dust sublimation radius by focussing on the infrared regime where the relationship between luminosity and the prominence of the 3–5 μm bump may be key. To investigate this further, we apply the 3D hydrodynamic wind model of Everett (2005) to predict the infrared spectral energy distributions of quasars. The presence of the 3–5 μm bump and strong, broad silicate features can be reproduced with this dynamical wind model when radiation driving on dust is taken into account.

1. Introduction

The torus was introduced by Antonucci & Miller (1985) to explain the revelation from spectropolarimetry that Type 2 (narrow-line) Seyfert galaxies can look like Type 1 (broad-line) Seyferts along different lines of sight. Since that discovery, the torus' primary purpose has been to obscure the broad-line region, but it also serves to explain the near- and mid-infrared (IR) emission observed in the vast majority of quasars whose spectral energy distributions (SEDs) indicate dust heated to near sublimation temperatures, presumably by the accretion-disk continuum.

Typically, the torus has been modeled as a static, axisymmetric structure (e.g., Pier & Krolik 1992) that may have condensations (clumps or clouds) within it (e.g., Nenkova et al. 2008). A notable exception to this paradigm is the dusty wind model of Königl & Kartje (1994), who started with a magneto-hydrodynamic (MHD) wind, and added in radiation driving on grains beyond the dust sublimation radius. They were motivated in part by the large scale-height of the obscurer required by the observed Seyfert 1 to Seyfert 2 ratio, the inevitability of radiation driving in the presence of such a strong source of UV photons, and the apparent luminosity-dependent covering fraction of the torus (Lawrence 1991). Since then others (e.g., Elitzur & Shlosman 2006) have also incorporated some wind component into their models, and/or the effects of IR radiation-pressure in inflating the dusty medium (e.g., Dorodnitsyn et al. 2011). The questions remains: how to test for the existence of this dusty wind?

In the UV, wind signatures are clearly evident in the broad resonance lines of high ionization species such as C iv. While most apparent in classic P-Cygni-like broad absorption lines (e.g., Lynds 1967), the asymmetries in the same broad emission lines

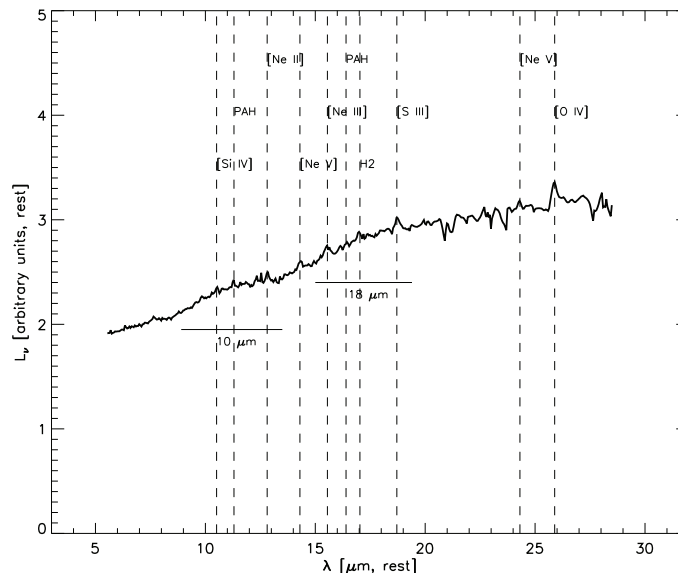


Figure 1. A composite IR spectrum made from ~ 50 luminous SDSS quasars from the *Spitzer* IRS archive. Prominent emission features are labeled; the horizontal bars indicate the approximate location of the broad silicate emission bumps. From Hill et al. (in preparation).

are also evidence for winds (e.g., Leighly 2004; Kruczek et al. 2011). The most natural mechanism for accounting for the high velocities ($\sim 10^4$ km s $^{-1}$) of the outflows is resonance-line driving by UV continuum photons.

Unlike the clear wind signatures in the UV, quasar IR spectra are characterized by broad features, such as the silicate emission bumps from the vibrational stretching and bending modes of the grains at 10 and 18 μ m, respectively (see Figure 1). The widths and peaks of the silicate bumps are affected by the grain size distribution, and so extracting information on the velocity of the emitting grains is impossible given the uncertainties in the inherent shape of the bumps. Narrow atomic features in the IR are from forbidden lines such as [O IV] and [Ne V] generated in low density, photoionized gas in the inner parts of the narrow-line region. Clear spectral signatures of a dusty wind are therefore elusive.

2. Luminosity Dependence of the 3–5 μ m Bump

In the UV, the maximum possible terminal velocity of outflows seen in absorption appears to be set by the UV luminosity (Laor & Brandt 2002; Ganguly et al. 2007). This makes sense for a radiation-driven UV outflow; a high UV photon density has the ability to transfer more momentum to the ionized wind. While this particular mechanism is not relevant in the IR, spectral features in this regime whose strength depends on luminosity are potentially fruitful for looking for evidence of the wind from the dust. One such feature is the 3–5 μ m bump, which can be successfully modeled as a blackbody with a temperature of 1200–1500 K (e.g., Barvainis 1987; Deo et al. 2011). These

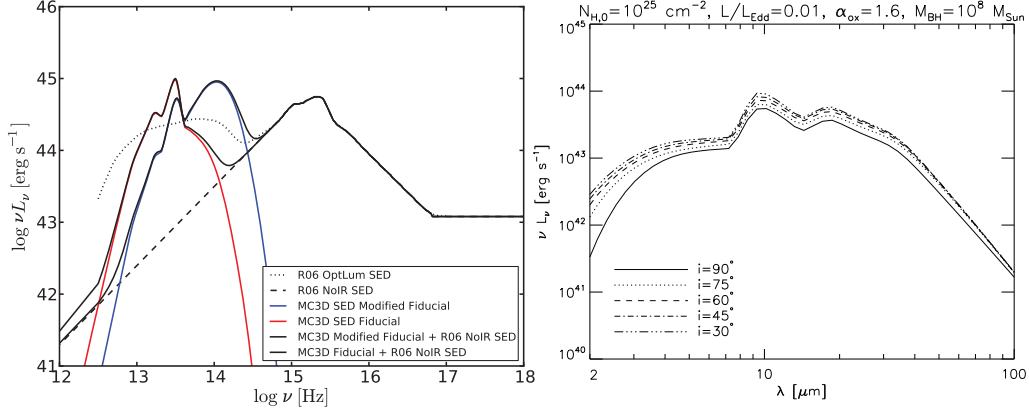


Figure 2. *Left:* IR to X-ray quasar SEDs as follows: the empirical R06 composite of optically luminous quasars (dotted); the input incident accretion disk continuum (dashed); the output IR SED for the characteristic model (red solid); the summed output IR SED and input incident accretion disk continuum (solid black). A characteristic model with a smaller dust-sublimation radius shows an SED (blue solid) peaking in the near-IR. As the dust-sublimation radius is increased the SED power decreases in the near-IR and the peak emission shifts to longer wavelengths; small dust sublimation radii are required to generate strong 3–5 μm bump emission. *Right:* The output IR SEDs generated by the wind models; different line styles are used to distinguish the observed inclination angle, i , with respect to the normal to the accretion disk. The power and shape of the SED is not particularly sensitive to the angle, indicating that the wind is optically thin to IR radiation for $\lambda \geq 8 \mu\text{m}$. The short wavelength emission increases with smaller inclination angle. This effect could contribute to relatively stronger 3–5 μm emission in more luminous objects because their more radial dusty winds reveal the hottest dust in a larger range of inclination angles. Figures from Keating et al. (2012).

temperatures are interesting because they are near the grain sublimation temperature of graphites, but higher than the grain sublimation temperature of silicates. Edelson & Malkan (1986) first noted that this feature becomes stronger at higher luminosities. Gallagher et al. (2007) confirmed this trend with a much larger sample of SDSS quasars with *Spitzer* IRAC + MIPS photometry by searching for convex spectra between 1 and 8 μm ; the amount of spectral curvature was significantly correlated with luminosity.

The increasing prominence of the 3–5 μm bump can be qualitatively understood in a wind paradigm, because more luminous quasars will have more radial IR outflows. Assuming an accretion disk is the source of the optical through X-ray continuum, the dust-driving continuum will always be interior to (and significantly more compact than) the dusty wind, and thus act in the radial direction. In this scenario, the hottest dust is visible from a larger range of inclination angles in luminous objects. In the UV, an ionized wind launched from the accretion disk at small radii ($\sim 10^{16}$ cm) could have a significant vertical component to its acceleration. This geometric effect can naturally account for the larger observed fraction of BAL quasars (seen when looking through the UV wind) compared to type 2 quasars (seen when the broad-line region is blocked by thick, dusty material).

3. The MHD Dusty Wind Model

To investigate the interplay of radiation driving and the IR SED, we have developed a dynamical model of the torus as a dusty wind launched by MHD forces and by radiation pressure from the accretion disk continuum. The dusty wind generated in this manner can cover a large fraction of the sky as seen from the central black hole. This model has the benefit of being more self-consistent than static torus models and including the important physics of motion around the black hole and radiative acceleration. Ultimately, we wish to use this model to understand how the physical properties of dusty winds in quasars correlate with their observable spectral signatures in the IR.

The model and its corresponding code has been expanded from its original form (described in Königl & Kartje 1994) by Everett (2005), where a comprehensive account of the model's components and key equations are described. We advance on Everett (2005) by adding the continuum opacity of ISM dust grains, as specified by the ISM dust model (Mathis et al. 1977; van Hoof et al. 2004) in Cloudy (Ferland et al. 1998).

The radiation pressure on the dust from the central source is very strong – even for cases where $L/L_{\text{Edd}} = 0.1$, it is approximately 10 times the force required to unbind dust from the gravitational potential (Everett et al. 2009). Dust grains absorb radially streaming photons originating from the accretion disk, and then cool by radiating isotropically. The force, felt by the dust particles due to conservation of momentum, feeds back on the wind structure by bending the magnetic wind from a vertical to more radial structure. The radiative force works in conjunction with the magneto-centrifugal forces to accelerate the wind flow and therefore modifies the structure of the outflow.

After iterating the MHD+radiation pressure calculations to set up the structure of the wind, we use the Monte Carlo radiative-transfer code MC3D (Wolf 2003) to send rays through the wind and predict the observed IR SEDs. The input parameters for the wind such as Eddington ratio (L/L_{Edd}), black hole mass (M_{BH}), and illuminating continuum (the empirical optical-to-X-ray composite of Richards et al. 2006, hereafter R06) are varied to investigate their effects on the output SED.

4. Principal Results

With input parameters appropriate for luminous quasars (luminosity of the incident continuum: $L_{\text{bol}} \sim 10^{46} \text{ erg s}^{-1}$; $L/L_{\text{Edd}} = 0.1$; $M_{\text{BH}} = 10^8 M_{\odot}$; column density at the base of the wind: $N_{\text{H},0} = 10^{25} \text{ cm}^{-2}$; and observer's inclination angle from the disk normal: $i = 60^\circ$), we can produce reasonable IR SEDs with approximately the right shape and luminosity ($L \approx 10^{43} - 10^{45} \text{ erg s}^{-1}$) as expected from the R06 composite of optically luminous SDSS quasars (see Figure 2). This is a promising result for a relatively simple model given that we have not attempted any fitting.

A benefit to our model is that we are able to see directly the effects of various physical parameters on the final IR SED, which ultimately will allow us to understand the physical properties of the torus itself. By determining which physical parameters have an observable effect on the IR SEDs, and narrowing them down so that we generally reproduce the power expected, we have established a reasonable starting point from which we can expand and further refine our model.

5. Future Work

In the near future, we plan to implement a more sophisticated treatment of dust grains that takes into account the different sublimation temperatures of graphite and silicate. The luminosity dependence of emission from the hottest grains — graphites — is promising as a means of demonstrating the connection between radiative driving of grains, wind geometry, and the observed SED. We expect that radiation pressure must be important, because otherwise the luminosity dependence of the torus covering fraction and of the 3–5 μm emission is hard to understand.

Our ultimate goal is to generate a library of realistic, IR SEDs that can be compared with *Spitzer* IRS observations of quasars. We aim to determine (1) if reasonable input properties (e.g., the input continuum shape, L/L_{Edd} , and M_{BH}) result in SEDs that match in detail those observed, and more ambitiously, (2) how to use the empirical IR SEDs to independently constrain the unknown physical properties of quasars.

References

- Antonucci, R. R. J., & Miller, J. S. 1985, *ApJ*, 297, 621
 Barvainis, R. 1987, *ApJ*, 320, 537
 Deo, R. P., Richards, G. T., Nikutta, R., Elitzur, M., Gallagher, S. C., Ivezić, Ž., & Hines, D. 2011, *ApJ*, 729, 108. 1101.2855
 Dorodnitsyn, A., Bisnovatyi-Kogan, G. S., & Kallman, T. 2011, *ApJ*, 741, 29. 1108.3766
 Edelson, R. A., & Malkan, M. A. 1986, *ApJ*, 308, 59
 Elitzur, M., & Shlosman, I. 2006, *ApJ*, 648, L101. arXiv:astro-ph/0605686
 Everett, J. E. 2005, *ApJ*, 631, 689. arXiv:astro-ph/0506321
 Everett, J. E., Gallagher, S. C., & Keating, S. K. 2009, in *The Monster's Fiery Breath: Feedback in Galaxies, Groups, and Clusters*, edited by S. Heinz & E. Wilcots, vol. 1201 of American Institute of Physics Conference Proceedings, 56
 Ferland, G. J., Korista, K. T., Verner, D. A., Ferguson, J. W., Kingdon, J. B., & Verner, E. M. 1998, *PASP*, 110, 761
 Gallagher, S. C., Richards, G. T., Lacy, M., Hines, D. C., Elitzur, M., & Storrie-Lombardi, L. J. 2007, *ApJ*, 661, 30. arXiv:astro-ph/0702272
 Ganguly, R., Brotherton, M. S., Cales, S., Scoggins, B., Shang, Z., & Vestergaard, M. 2007, *ApJ*, 665, 990. 0705.1546
 Königl, A., & Kartje, J. F. 1994, *ApJ*, 434, 446
 Kruczek, N. E., Richards, G. T., Gallagher, S. C., Deo, R. P., Hall, P. B., Hewett, P. C., Leighly, K. M., Krawczyk, C. M., & Proga, D. 2011, *AJ*, 142, 130. 1109.1515
 Laor, A., & Brandt, W. N. 2002, *ApJ*, 569, 641
 Lawrence, A. 1991, *MNRAS*, 252, 586
 Leighly, K. M. 2004, *ApJ*, 611, 125. arXiv:astro-ph/0402452
 Lynds, C. R. 1967, *ApJ*, 147, 396
 Mathis, J. S., Ruml, W., & Nordsieck, K. H. 1977, *ApJ*, 217, 425
 Nenkova, M., Sirocky, M. M., Ivezić, Ž., & Elitzur, M. 2008, *ApJ*, 685, 147. 0806.0511
 Pier, E. A., & Krolik, J. H. 1992, *ApJ*, 401, 99
 Richards, G. T., Lacy, M., Storrie-Lombardi, L. J., Hall, P. B., Gallagher, S. C., Hines, D. C., Fan, X., Papovich, C., Vanden Berk, D. E., Trammell, G. B., Schneider, D. P., Vestergaard, M., York, D. G., Jester, S., Anderson, S. F., Budavári, T., & Szalay, A. S. 2006, *ApJS*, 166, 470. arXiv:astro-ph/0601558
 van Hoof, P. A. M., Weingartner, J. C., Martin, P. G., Volk, K., & Ferland, G. J. 2004, *MNRAS*, 350, 1330. arXiv:astro-ph/0402381
 Wolf, S. 2003, *Computer Physics Communications*, 150, 99. arXiv:astro-ph/0207374